SUSY Higgs Sector

Yasuhiro Okada (KEK)

@コライダー物理研究会.
東大. May 19. 2001

Higgs Sector の物理

- Electroweak symmetry breaking の機構
- gauge boson, fermion の質量生成

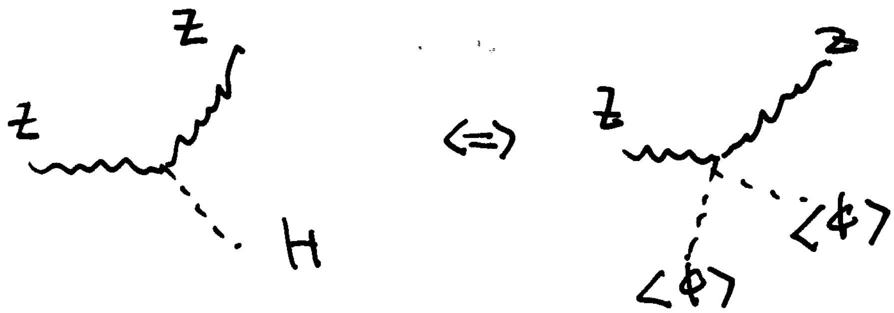

$$m_Z = \frac{\sqrt{g^2+g'^2}}{2}\langle\phi\rangle$$

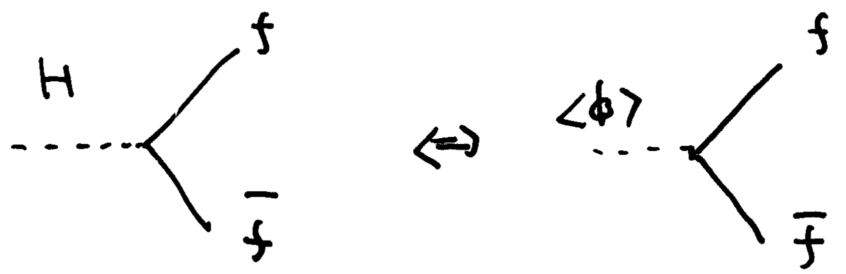

$$m_f = \frac{y_f\langle\phi\rangle}{\sqrt{2}}$$

- Higgs Potential

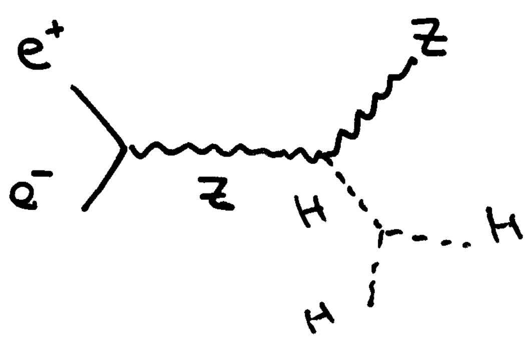

$$V(\phi) = -\mu^2|\phi|^2 + \lambda|\phi|^4$$

SUSY model，特に minimal supersymmetric Standard model (MSSM) では．Higgs Sector は特徴的な構造を持つ．

- Particle content
- mass bound
- Coupling constant.

- SUSY model の check point

- SUSY 理論の parameter を決める．

定量的検証．

[1] Higgs boson mass in MSSM

Higgs boson mass in the Standard Model

$$m_h = \sqrt{2\lambda}\, v$$

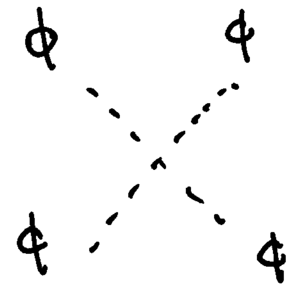

λ, $\quad V = -\mu^2|\phi| + \lambda|\phi|^4$

Light Higgs boson ⟺ Weakly interacting

Heavy Higgs boson ⟺ Strongly interacting

Running coupling constant. λ, y_t, g, g'

$$\mu \frac{d}{d\mu}\lambda = \frac{1}{(4\pi)^2}\left\{24\lambda^2 + 12 y_t \lambda - 6 y_t^4 + \cdots\right\}$$

↑ gauge coupling constant による項

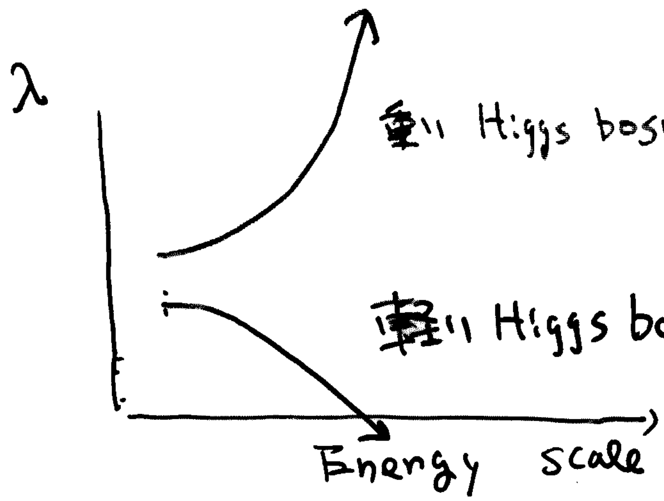

Vacuum instability at $\phi \sim O(\mu)$

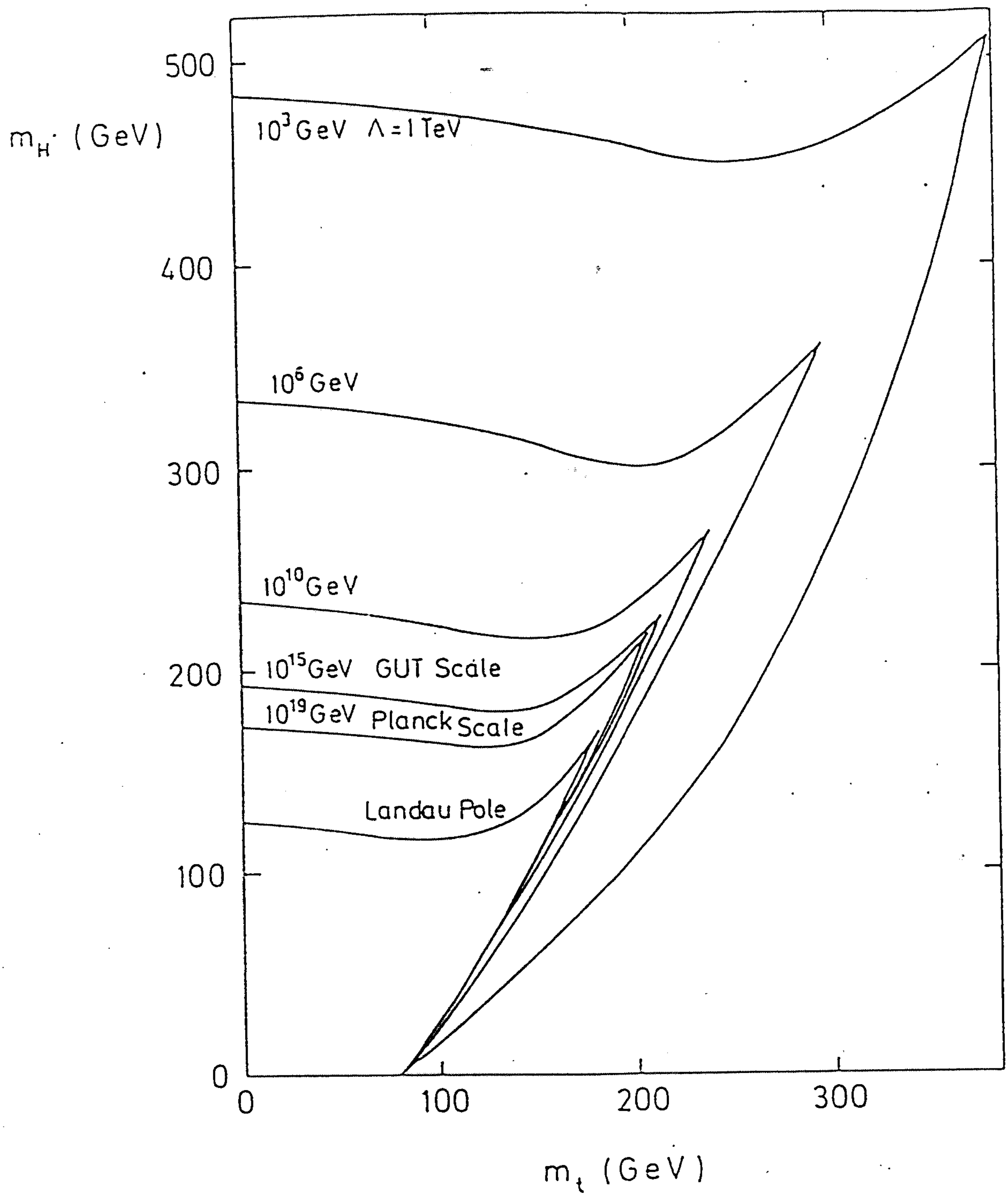

Fig. 2. The allowed parameter space of m_H and m_t for various embedding scales Λ. Allowed is the area around the origin bounded by the various curves. The curve entitled with Landau pole is identical to the curve of Beg et al. The horizontal lines come from avoiding triviality and the vertical lines are determined from $\lambda(t)$ becoming negative at scales lower than Λ

cutoff scale $\Lambda = 10^{19}$ GeV まで SM が成立する

と考えると

$$130\,\mathrm{GeV} \lesssim m_H \lesssim 180\,\mathrm{GeV}$$

ただし 我々の 真空が meta-stable で、その

寿命が 宇宙年齢より大きいとすると lower bound

は 少し 小さくなる。

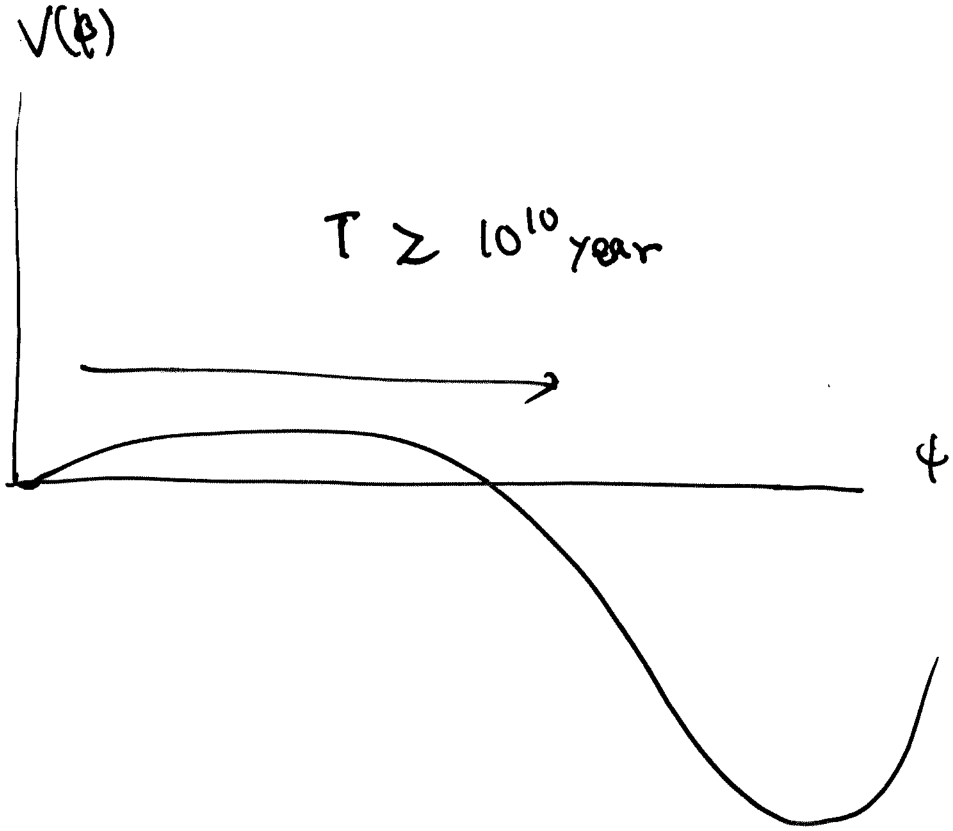

G. Ishidori, G. Ridolfi, A. Strumia hep-ph/0104016

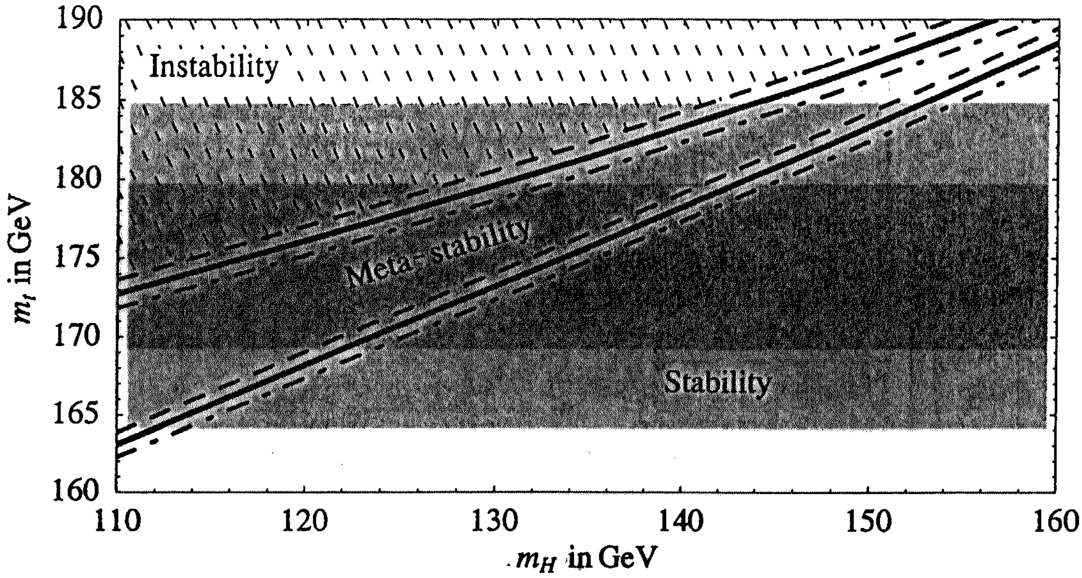

Figure 4: *Metastability region of the Standard Model vacuum in the* (m_H, m_t) *plane, for* $\alpha_s(m_Z) = 0.118$ *(solid curves). Dashed and dot-dashed curves are obtained for* $\alpha_s(m_Z) = 0.118 \pm 0.002$*. The shaded area indicates the experimental range for* m_t*. Sub-leading effects could shift the bounds by* ± 2 GeV *in* m_t*.*

Final result for the gauge sector

Summing the regularized gauge and Goldstone corrections, we finally obtain

$$\Delta S_{\rm gauge} = 2 f_g\left(\frac{g_2^2}{|\lambda|}\right) + f_g\left(\frac{g_Z^2}{|\lambda|}\right) + f_h^{(2)} + 3 f_h^{(3)} , \tag{4.58}$$

where

$$f_h^{(3)} = \lim_{g\to 0}\left[(\Delta S'_{j=0} - \ln R) + \Delta S_{j>0} - \Delta S^{[2]}\right]^A \approx 2 \tag{4.59}$$

and

$$f_g\left(\frac{g^2}{|\lambda|}\right) = \left[(\Delta S'_{j=0} - \ln R) + \Delta S_{j>0} - \Delta S^{[2]}\right]^A - f_h^{(3)} , \tag{4.60}$$

so that $f_g(0) = 0$. The function f_g, obtained by means of numerical integration, is plotted in Fig. 2. The constants $f_h^{(2)}, f_h^{(3)}$ can finally be combined with $f_h^{(1)}$ in Eq. (4.22) and with the translation prefactors $S_0^2/(2\pi)^2$ to yield

$$f_h = f_h^{(1)} + f_h^{(2)} + 3 f_h^{(3)} - \ln\frac{16\pi^2}{9\lambda^2} = \frac{7}{2}\ln|\lambda| - 8 \pm 1 . \tag{4.61}$$

This numerical estimate has been obtained with $Rv = 10^{-14}$, but it is very mildly sensitive to the value of Rv.

MSSM

SM の最も簡単な SUSY extension

quark / lepton	$\Leftrightarrow$	squark / slepton
gluon	$\Leftrightarrow$	gluino
EW gauge boson W^μ, B^μ; Higgs field H_1, H_2	$\Leftrightarrow$	$\chi_i^\pm$ $i=1,2$ chargino; χ_i^0 $i=1-4$ neutralino

◎ Higgs Sector の特徴

① Type II Two Higgs doublet model

$$\mathcal{L}_{Yukawa} = y_u H_2 \bar{u}_R q_L + y_d H_1 \bar{d}_R q_L + y_e H_1 \bar{e}_R l_L + h.c.$$

・SUSY invariance を保ってすべての quark, lepton に質量を与えるためには、2種類の Higgs doublet field を用意しなくてはならない

・2HDM のときのみ gauge coupling unification がうまくいく。

② 軽い CP-even Higgs boson の質量に上限がある。

Physical Higgs States
- CPeven h, H $(m_h \leq m_H)$
- CPodd A
- Charged Higgs $H^{\pm}$

Higgs Potential

$$V(H_1, H_2) = m_1^2 |H_1|^2 + m_2^2 |H_2|^2 - m_3^2 (H_1 H_2 + H_1^* H_2^*)$$
$$+ \frac{g^2}{8} (H_1^\dagger \tau^a H_1 + H_2^\dagger \tau^a H_2)^2$$
$$+ \frac{g'^2}{8} (|H_1|^2 - |H_2|^2)^2$$

+ One loop potential

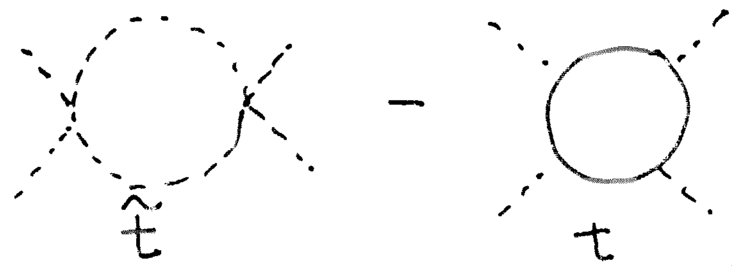

$$\simeq \frac{6}{16\pi^2} y_t^4 |H_2|^4 \ln \frac{m_{stop}^2}{m_t^2}$$

$$\Rightarrow m_h^2 \lesssim m_Z^2 \cos^2 2\beta + \frac{6}{(2\pi)^2} \frac{m_t^4}{v^2} \ln \frac{m_{stop}^2}{m_t^2}$$

$$\tan\beta \equiv \frac{\langle H_2^0 \rangle}{\langle H_1^0 \rangle}$$

$$m_h \lesssim 130 \text{ GeV}$$

Lightest CP even Higgs boson mass in MSSM

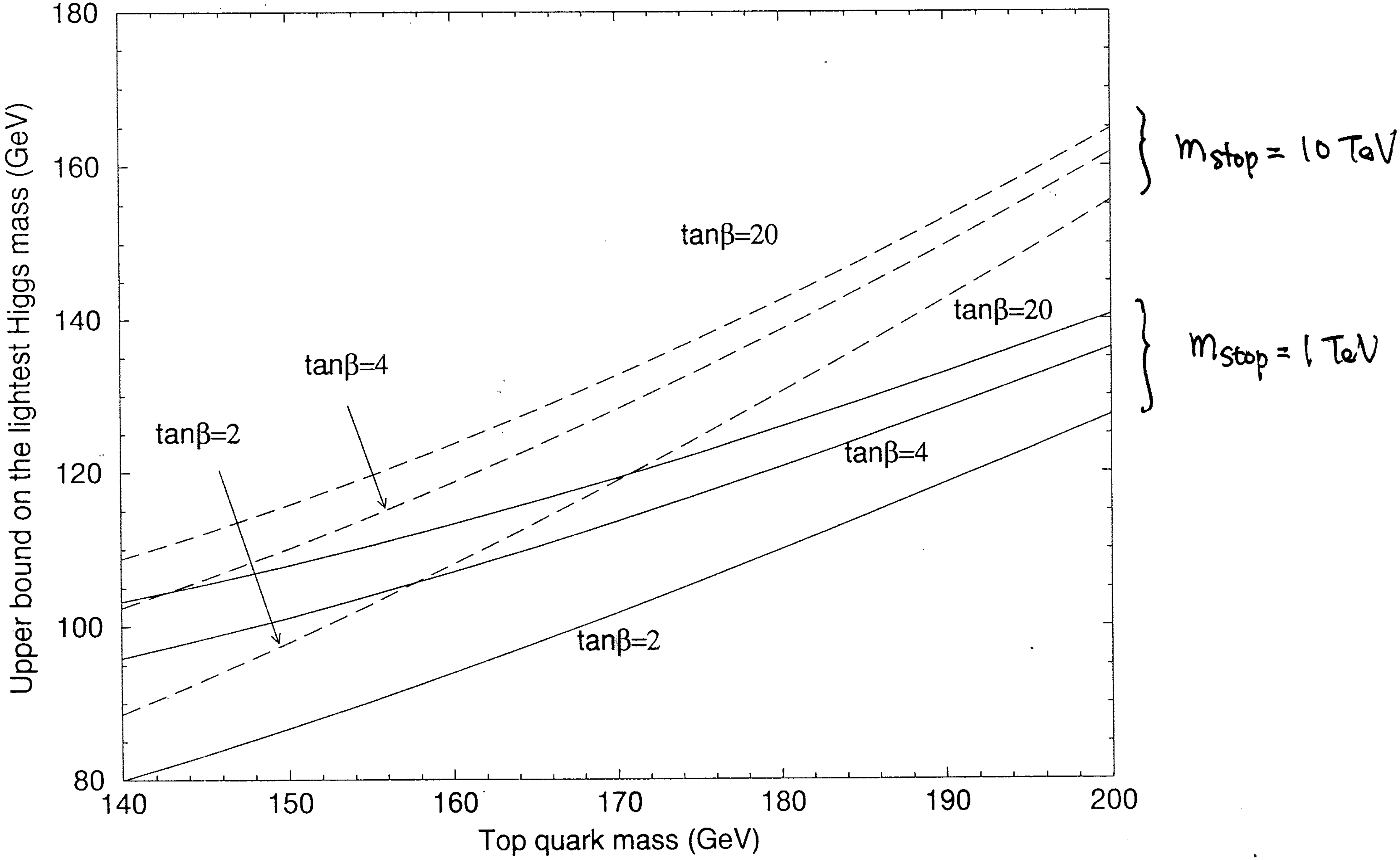

大きな補正を受ける理由.

SUSY particle が m_{SUSY} の質量を持っている

$m_{SUSY} \gg m_Z$ と仮定してみる.

Energy scale $\gg m_{SUSY}$ SUSY の破れの効果は小さい

Energy scale $\lesssim m_{SUSY}$ SUSY 粒子の効果は decouple して effective に SM にみえる.

Higgs self coupling constant の running.

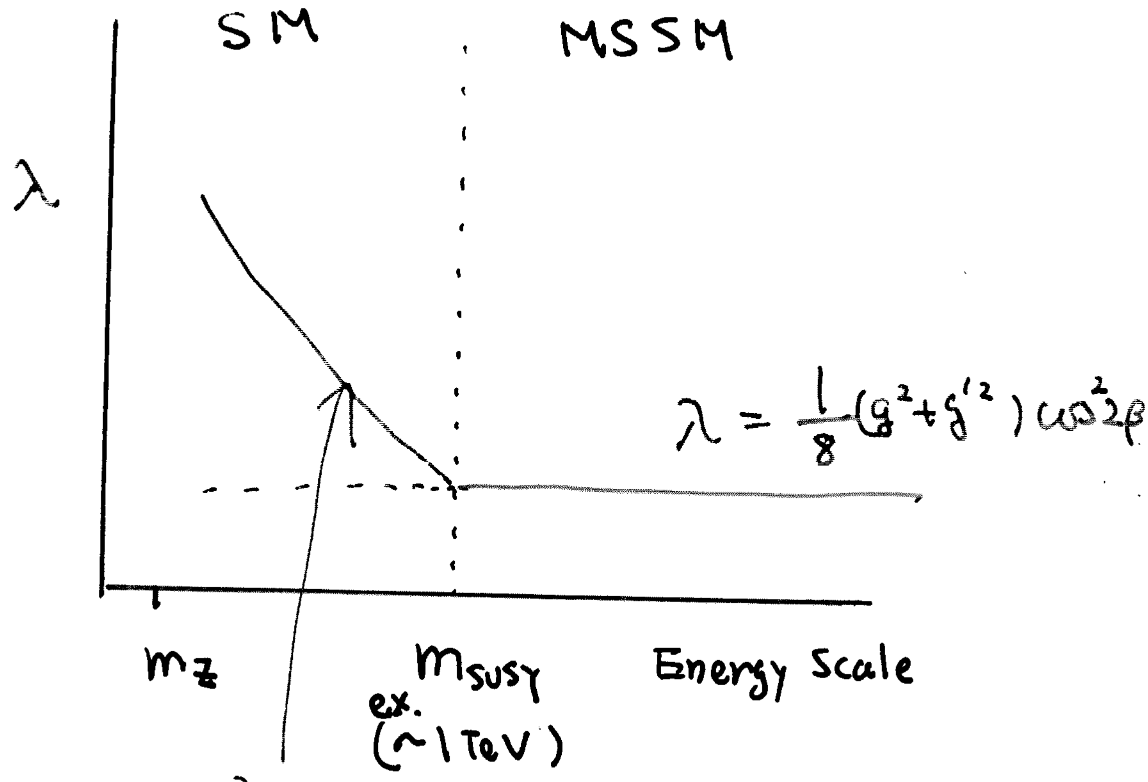

$$\mu \frac{d\lambda}{d\mu} = \frac{1}{(4\pi)^2}\left\{24\lambda^2 - 6 y_t^4 + \cdots\right\}$$

"Breakdown of SUSY relation"

重い Higgs Boson　($H, A, H^{\pm}$)

MSSM の Higgs Sector を指定するパラメーター

$m_1^2,\ m_2^2,\ m_3^2$, ⊕ $g,\ g'$ ⊕ $m_t,\ m_{stop}$

$\Rightarrow\ m_A,\ \tan\beta,\ m_t,\ m_{stop}$ ⊕ $\underbrace{m_Z,\ g,\ g'}_{\text{SM の parameter}}$

ほんとうは 1loop potential のパラメーターはもっと多い。($m_{\tilde{t}_1},\ m_{\tilde{t}_2},\ A_t,\ \mu,\ m_{\tilde{b}},\cdots$)

いったんこれらのパラメーターを指定すると、他の Higgs boson の質量と CP-even Higgs boson の mixing angle α は計算できる。

$$\mathrm{Re}\,H_1^0 = (v\cos\beta - h\sin\alpha + H\cos\alpha)\frac{1}{\sqrt{2}}$$

$$\mathrm{Re}\,H_2^0 = (v\sin\beta + h\cos\alpha + H\sin\alpha)\frac{1}{\sqrt{2}}$$

α: CP-even Higgs boson mixing angle

β: Vacuum angle

$$\left(\tan\beta \equiv \frac{\langle H_2^0\rangle}{\langle H_1^0\rangle}\right)$$

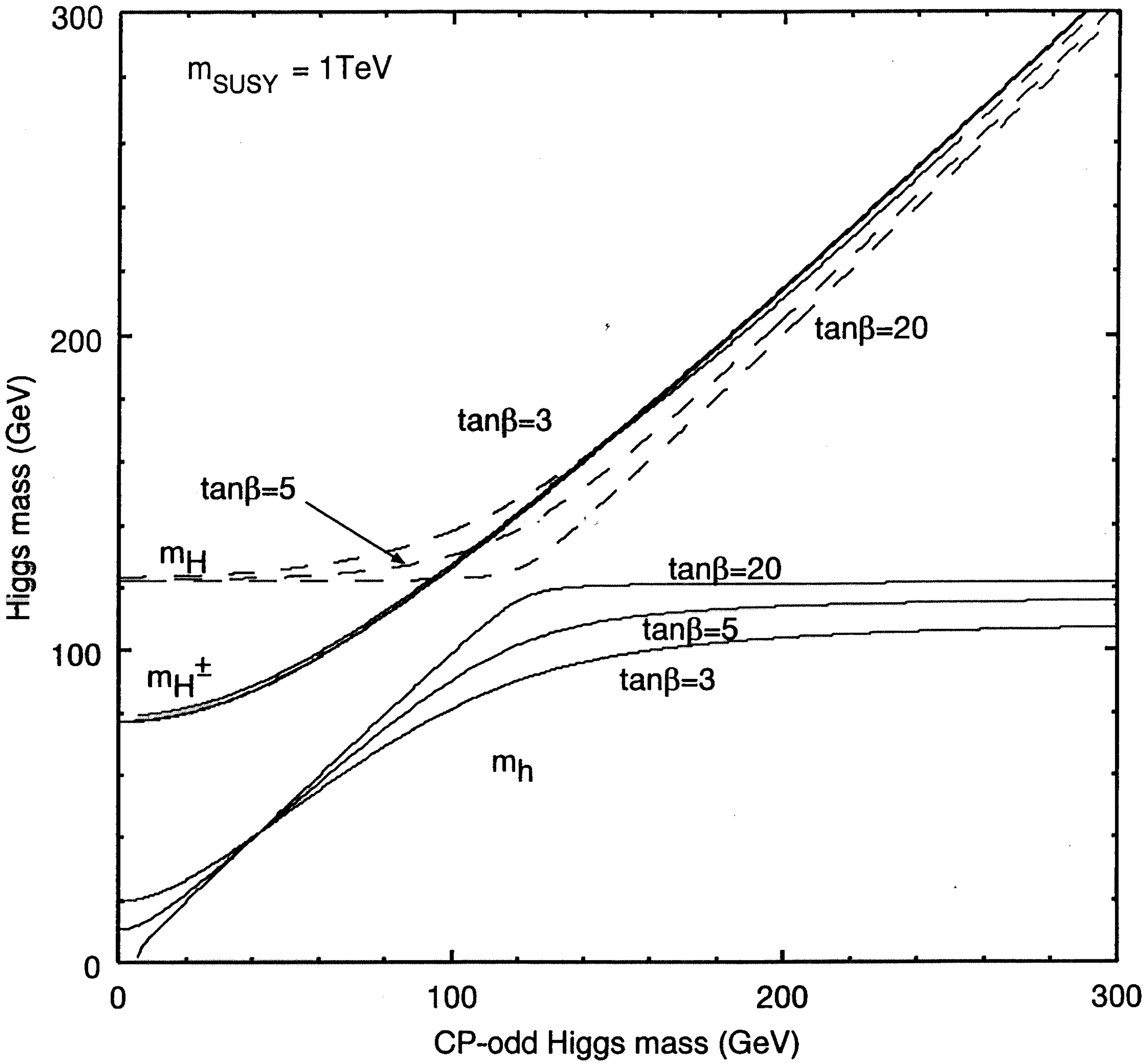

300
200
100
0
Higgs mass (GeV)
m_SUSY = 1TeV
tanβ=20
tanβ=3
tanβ=5
m_H
tanβ=20
tanβ=5
m_H±
tanβ=3
m_h
0
100
200
300
CP-odd Higgs mass (GeV)

2つの領域

① $m_A \lesssim 150\,\mathrm{GeV}$

2つのHiggs doubletがmixする

hとHの両方がEW symmetry breakingに関与する.

② $m_A \gtrsim 150\,\mathrm{GeV}$ (decoupling limit)

$h \to$ SM-like Higgs boson

$H, A, H^{\pm} \to$ 質量が縮退.

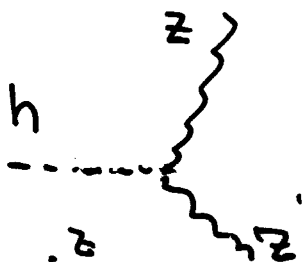

$\sin(\beta-\alpha) \to 1$

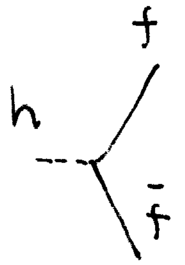

$y_f \to \frac{\sqrt{2} m_f}{v}$

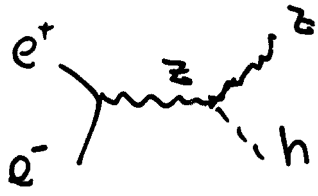

$\to 1$

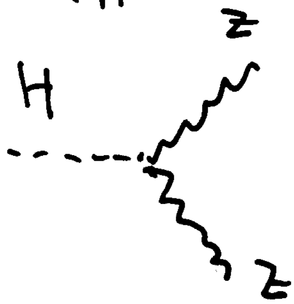

$\cos(\beta-\alpha) \to 0$

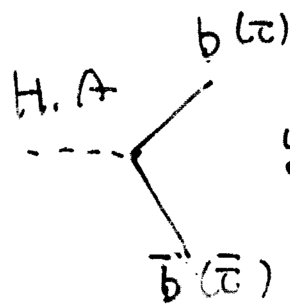

$y'_f \to \frac{\sqrt{2} m_f}{v} \tan\beta$

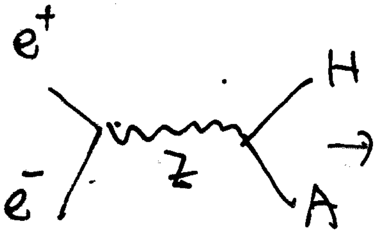

$\to 1$

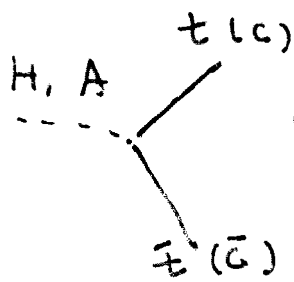

$y'_f \to \frac{\sqrt{2} m_f}{v} \cot\beta$

...

他の模型とのHiggs massの比較

・他の模型ではその模型がcutoff scale Λ まで成立すると仮定すると軽いHiggs bosonの質量の可能な領域を決めることができる.

① minimal SM

$$130\,\text{GeV} \lesssim m_H \lesssim 180\,\text{GeV}$$

$$(\Lambda = 10^{19}\,\text{GeV})$$

② Two Higgs doublet model.

$$100\,\text{GeV} \lesssim m_h \lesssim 180\,\text{GeV}$$

Decoupling limit, $(m_h \ll m_{H,A,H^\pm})$

$\Lambda = 10^{19}\,\text{GeV}$

③ MSSM + singlet Higgs field (NMSSM)

H_1, H_2, N

Higgs potential に tree level で新たな項が加わる

$$\Delta V = \lambda^2 |H_1 H_2|^2$$

$$m_h^2 \leq \frac{1}{2}\lambda^2 v^2 \sin^2 2\beta + m_Z^2 \cos^2 2\beta + \frac{6}{4\pi^2}\frac{m_t^4}{v^2}\ln\frac{m_{stop}^2}{m_t^2}$$

$m_h \lesssim 150\,\text{GeV}$. $(\Lambda = 10^{19}\,\text{GeV})$. $\tan\beta \simeq 2$ が許される.

S. Kanemura - T. Kasai - Y. Okada
1999

$\Lambda = 10^{19}$ GeV

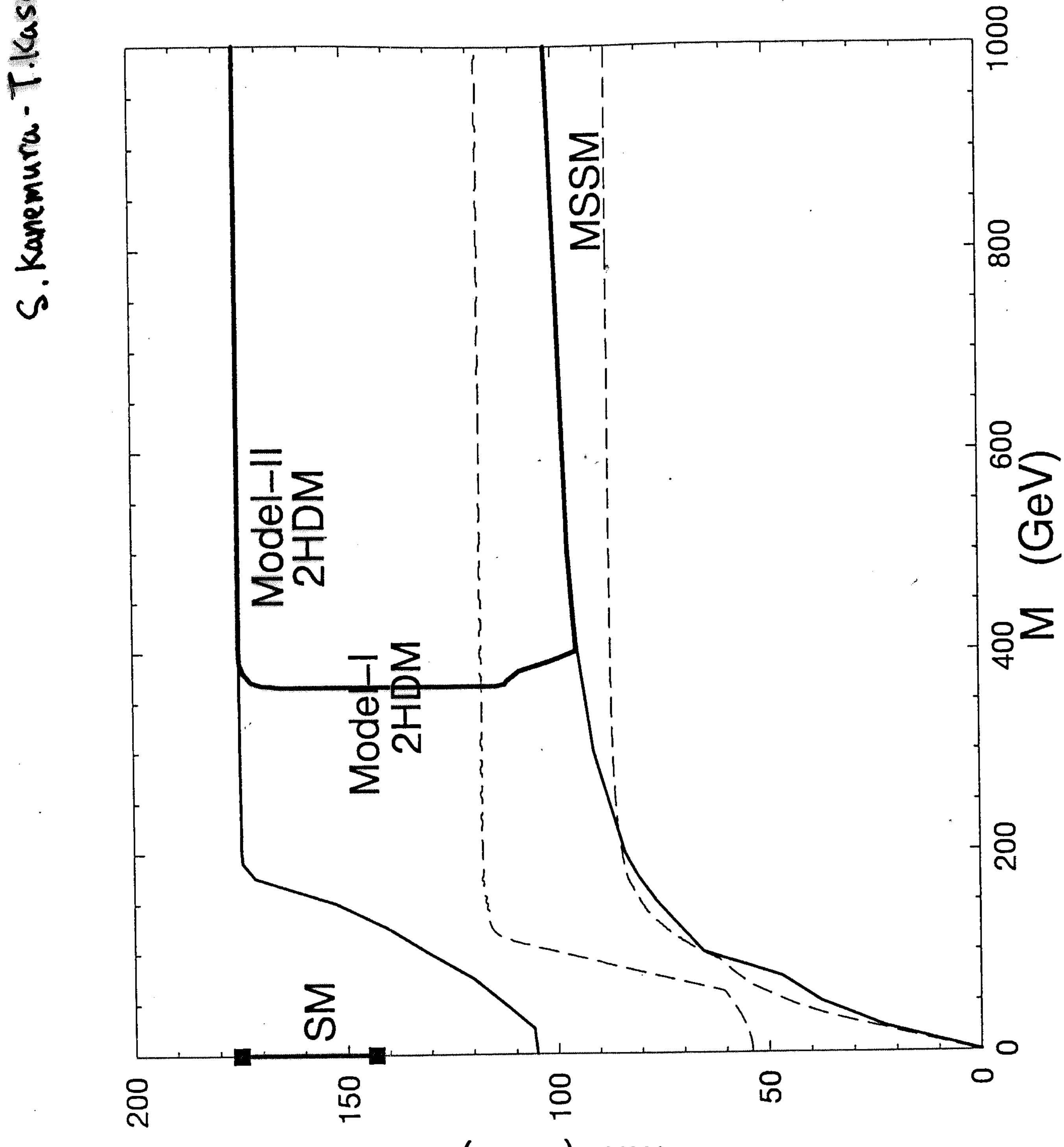

Fig. 4

④ Most General Higgs Sector

$$W = \lambda_1 H_1 H_2 S + \lambda_2 H_1 T_0 H_2 + \chi_1 H_1 T_1 H_1 + \chi_2 H_2 T_{-1} H_2$$

S: singlet Higgs field, T: triplet Higgs field

$m_h \lesssim 210$ GeV ($\Lambda = 10^{19}$ GeV)

⑤ MSSM ⊕ Vector-like matters

$m_h \lesssim 180$ GeV ($\Lambda = 10^{19}$ GeV)

J. R Espinosa. M Quirós 1998

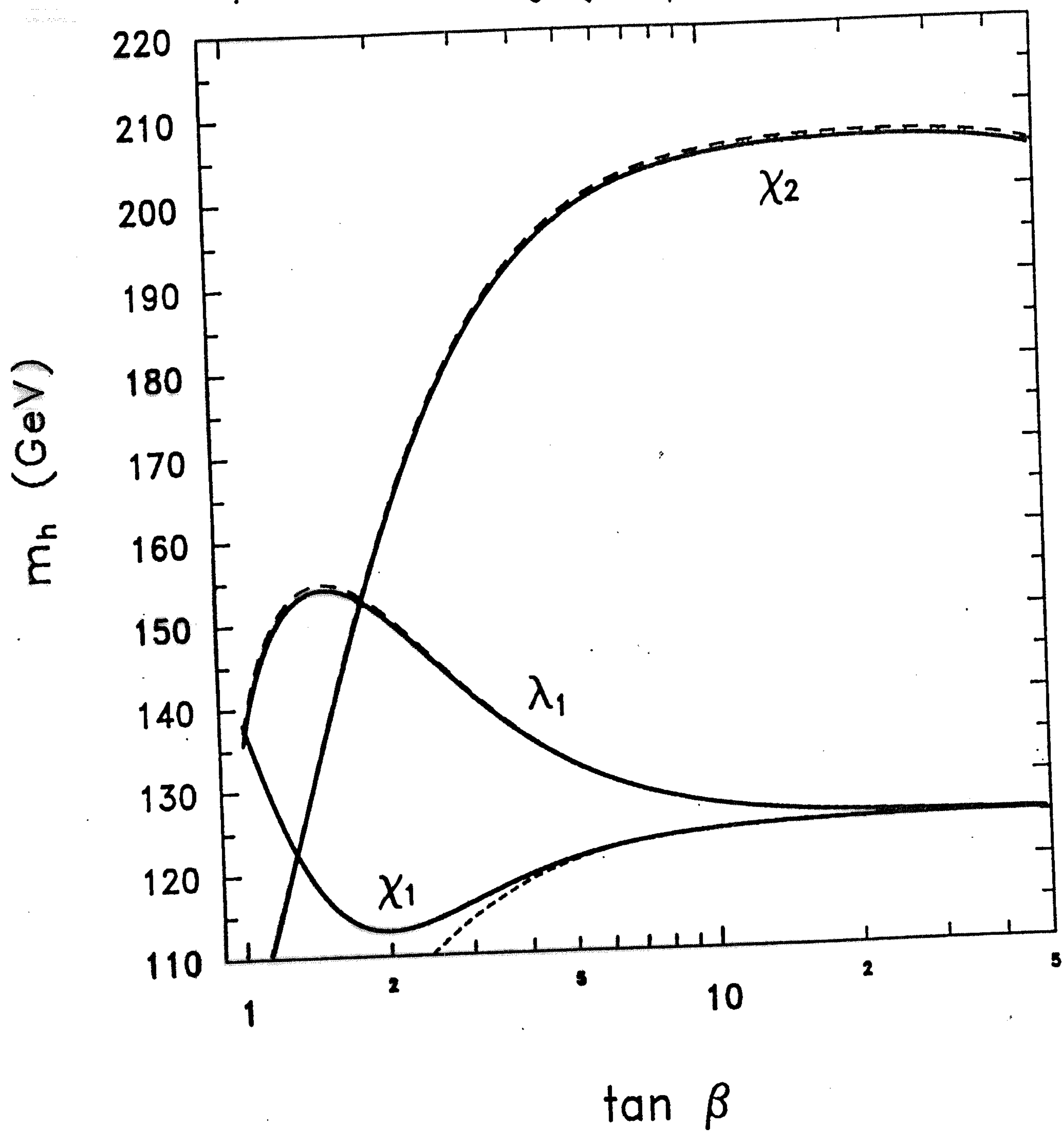

FIG. 2. Radiatively corrected upper bounds on m_h when different Yukawa couplings are present in the model and for different assumptions on the running of gauge couplings. The short-dashed line gives the upper bound in the MSSM.

Movoi Okada 1992

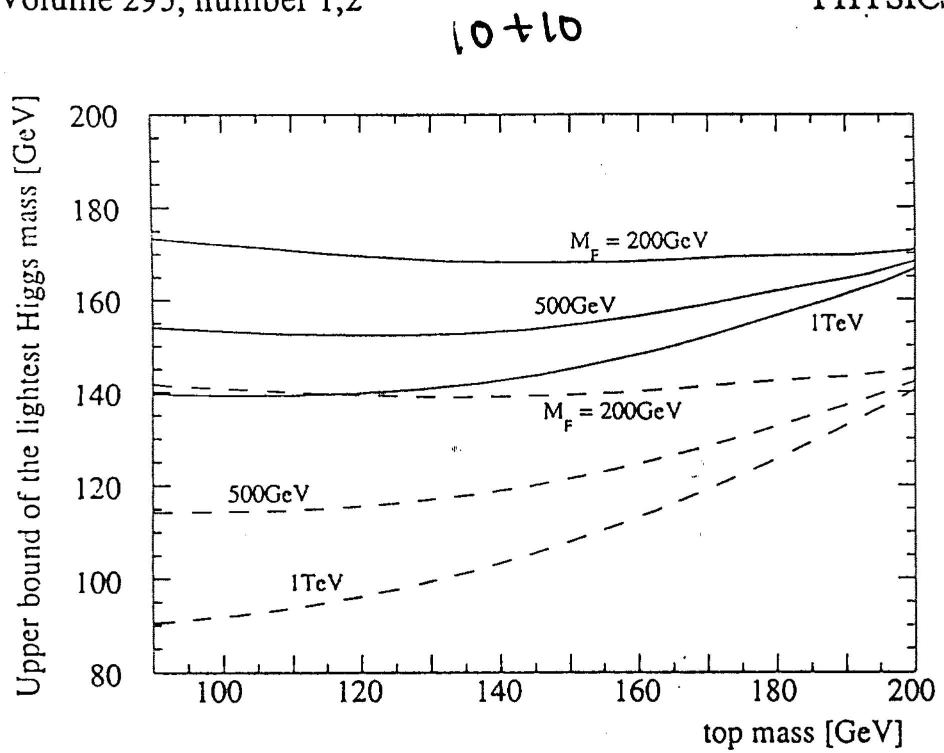

Fig. 1. The upper bound of the lightest neutral Higgs boson mass as a function of the top quark mass in the model with **10+10*** representation in SU(5). We take M_s=1 TeV and M_F=200 GeV, 500 GeV, 1 TeV. The solid lines correspond to the case that the a-parameters are equal to $\sqrt{6}$ and the dashed lines correspond to the case that the effects of the trilinear couplings are negligible.

tion from the extra families vanishes since the boson and fermion masses are degenerate. The figure shows

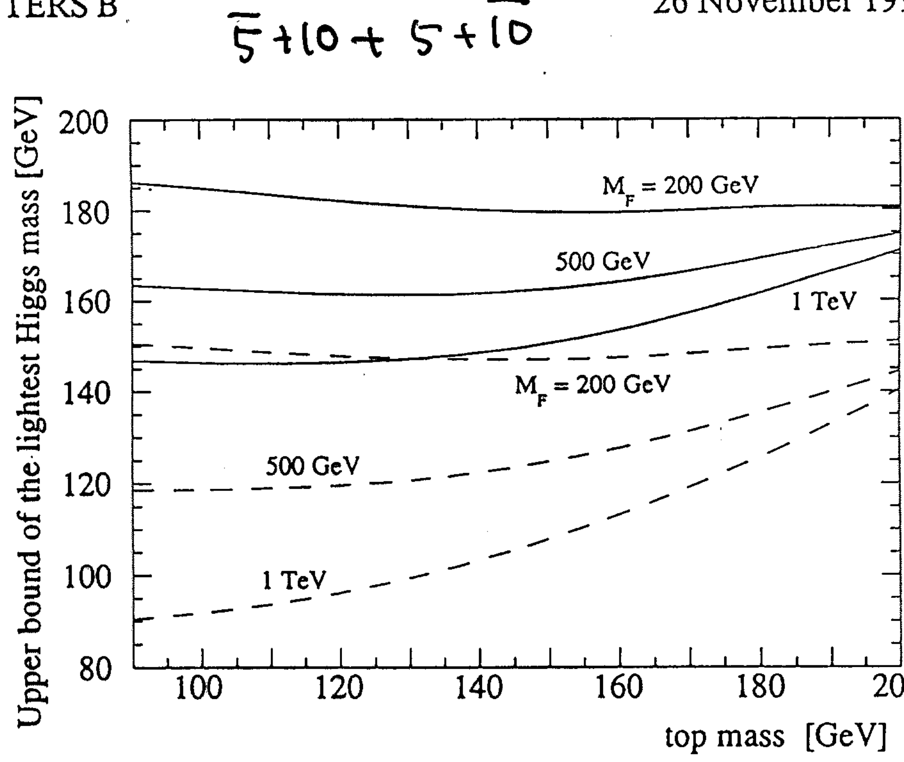

Fig. 2. The upper bound of the lightest neutral Higgs boson mass as a function of the top quark mass in the model with **5*+10+5+10***. All parameters are the same as in fig. 1.

where $y_{u'}$ and $y_{d'}$ are new Yukawa coupling constants, a very large value of $\tan\theta$ is not allowed from the experimental bounds of these masses. Therefore, we expect that the upper bound of M_{light} cannot be larger than those of the previous two models. For ex-

[2] Coupling constant measurement.

LHC や e^+e^- Linear Collider では.

Higgs boson と gauge boson, fermion の間の coupling constant やその比を測定することができる。

- SM と他の模型 (2HDM, MSSM, NMSSM etc) の区別をする
- ひとつの模型 (たとえば MSSM) で. パラメーターをどう決めるか.

- LHC

gluon fusion

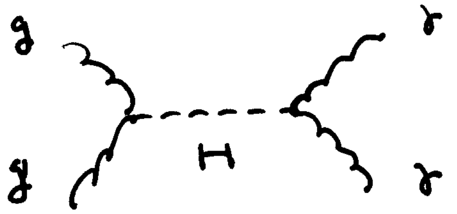

Weak boson fusion

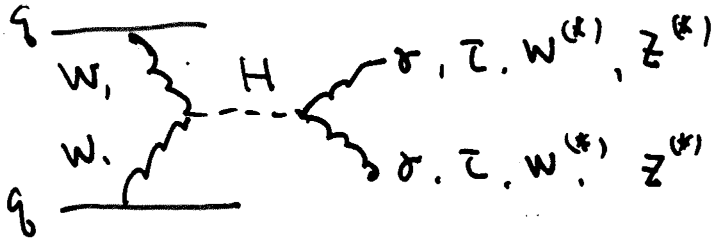

e^+e^- LC with $\sqrt{s} = 300 - 500$ GeV

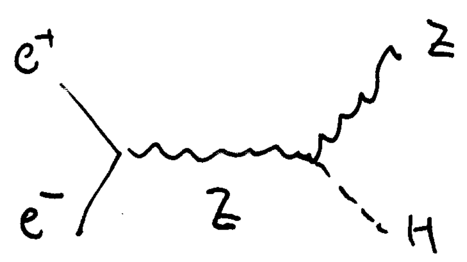

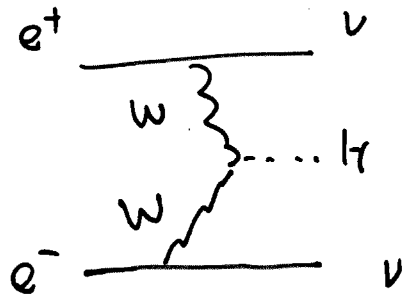

$H \to b\bar{b},\ gg,\ c\bar{c},\ \tau\bar{\tau},\ \gamma\gamma,\ WW^{(*)}$

Production cross section と Branching ratio

の精密測定

- Model-independent determination of coupling constants

S. Kyoura, Y. Okada

Higgs boson と up-type, down-type, charged-lepton,

gauge bosonとの coupling constant の SM とのずれを

次のようにパラメトライズする.

$$\mathcal{L} = x \frac{m_b}{v} h\bar{b}b + y\left(\frac{m_t}{v} h\bar{t}t + \frac{m_c}{v} h\bar{c}c\right)$$
$$+ z \frac{m_\tau}{v} h\bar{\tau}\tau + u\left(g m_W W_\mu W^\mu + \frac{\sqrt{g^2+g'^2}}{2} m_Z Z_\mu Z^\mu\right) h$$

- $x = y = z = u = 1$ SM
- $x = z = -\dfrac{\sin\alpha}{\cos\beta}$, $y = \dfrac{\cos\alpha}{\sin\beta}$, $z = \sin(\beta - \alpha)$

MSSM, Type-II 2HDM.

LHC

$$\frac{\Gamma(h\to gg)}{\Gamma(h\to WW)}$$:

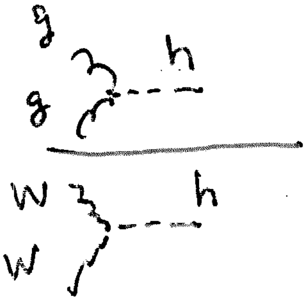

$\propto \left(\frac{y}{u}\right)^2$

$$\frac{\Gamma(h\to\tau\tau)}{\Gamma(h\to WW)}$$:

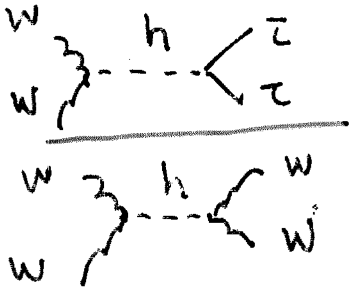

$\propto \left(\frac{z}{u}\right)^2$

10% level の coupling の決定

e^+e^- LC

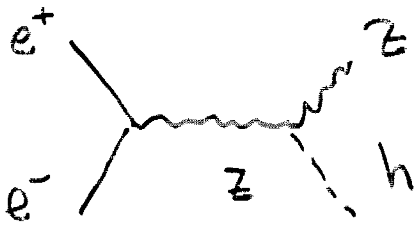

,

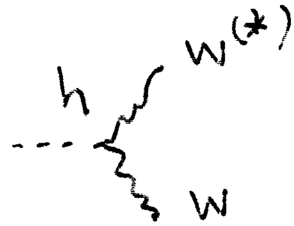

, u^2

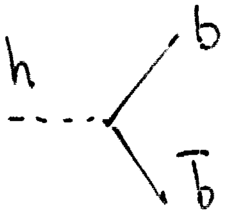

x^2

,

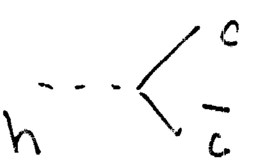

+

y^2

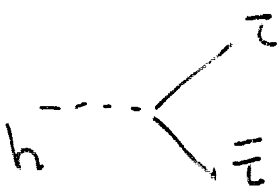

z^2

1-3.% level の coupling の決定

TABLE VII. Summary of the accuracy with which various ratios of partial widths can be determined with 200 fb^{-1} of data. The first two columns give the ratio considered and indicate the method by which it is measured. Y_Z/Y_W, for example, indicates a measurement of $\sigma B(H\rightarrow ZZ^*)/\sigma B(H\rightarrow WW^*)$ in gluon fusion, while X_i ratios correspond to weak boson fusion (see text for details). The statistical combination of several channels for a given width ratio is indicated by $\oplus$. 5% and 20% theoretical uncertainties for weak boson and gluon fusion cross sections affect the mixed gluon-weak boson fusion ratios only, which are needed for a measurement of Γ_g/Γ_W. The effect of this systematic error is indicated in the last line.

LHC
200 fb^{-1}

m_H		100	110	120	130	140	150	160	170	180
$z=\Gamma_Z/\Gamma_W$	Y_Z/Y_W			48%	29%	19%	17%	15%	20%	17%
	$\frac{Y_Z}{Y_\gamma}\frac{X_\gamma}{X_W}$			30%	21%	19%	23%			
	$\frac{Y_Z}{Y_W}\oplus\frac{Y_Z}{Y_\gamma}\frac{X_\gamma}{X_W}$			29%	19%	15%	14%	15%	20%	17%
Γ_γ/Γ_W	$\frac{Y_\gamma}{Y_W}\oplus\frac{X_\gamma}{X_W}$			16%	12%	11%	13%			
Γ_τ/Γ_W	$\frac{X_\tau}{X_W}$			15%	12%	14%	21%			
$\Gamma_\tau/\Gamma_\gamma$	$\frac{X_\tau}{X_\gamma}$	20%	16%	15%	16%	18%	27%			
Γ_g/Γ_W	$\frac{Y_\gamma}{X_\gamma}\oplus\frac{Y_W}{X_W}$	22%	18%	15%	13%	12%	13%	8%	9%	14%
	$\frac{Y_\gamma}{X_\gamma}\oplus\frac{Y_W}{X_W}\oplus 21\%$	30%	27%	25%	24%	24%	24%	22%	22%	25%

$$\Gamma_f=\Gamma(H\rightarrow \bar{f}f)=c_f\frac{g_{Hff}^2}{8\pi}\left(1-\frac{4m_f^2}{m_H^2}\right)^{3/2} m_H. \quad (9)$$

ments discussed in the previous section provide measurements of various combinations $\Gamma_i\Gamma_j/\Gamma$.

The production cross sections are subject to QCD correc-

ACFA LC Higgs W.G.

e^+e^- LC 500 fb^{-1}

$\sqrt{s}$	300 GeV	400 GeV	500 GeV
Δm_h (lepton-only)	80 MeV	—	—
Δm_h	40 MeV	—	—
$\Delta\sigma/\sigma$ (lepton-only)	2.1%	2.5%	2.9%
$\Delta\sigma/\sigma$	1.3%	—	—
$\Delta(\sigma_{h\nu\bar{\nu}}\cdot \mathrm{Br}(b\bar{b})$	2.0%	—	—
ZZH-coupling ΔZZH/ZZH	1.1%	1.3%	1.5%
WWH-coupling ΔWWH/WWH	1.6%	—	—
$\Delta\Gamma_{h^0}/\Gamma_{h^0}$	5.5%	12%	16%
Yukawa coupling $\Delta\lambda/\lambda$			
λ_b	2.8%	6.1%	8.1%
λ_τ	3.5%	—	—
λ_c	11.3%	13%	15%
λ_b/λ_τ	2.3%	—	—
λ_b/λ_c	11%	12%	14%
$\lambda_{up-type}$	4.1%	—	—
$\lambda_{down-type}/\lambda_{up-type}$	3.2%	—	—
$\Delta(\sigma\cdot\mathrm{Br})/(\sigma\cdot\mathrm{Br})$			
$h^0\to b\bar{b}$	1.1%	1.3%	1.7%
$h^0\to W^+W^-$	5.1%	12%	16%
$h^0\to\tau^+\tau^-$	4.4%	—	—
$h^0\to c\bar{c}+gg$	6.3%	—	—
$h^0\to c\bar{c}$	22%	23%	27%
$h^0\to gg$	10%	11%	13%
$h^0\to\gamma\gamma$	—	—	—
$h^0\to Z^0\gamma$	—	—	—

Table 8: Accuracy at $\sqrt{s}$ =300, 400 and 500 GeV with $\mathcal{L}$=500 fb^{-1} for 120 GeV CP-even Higgs at JLC. The Higgs boson of SM-like is used as an input.

6 Physics Outputs and Impacts in Models

Here we review the impacts of the Higgs studies at JLC, especially at phase-I, on the Higgs models, SUSY, GUT, and future generation of the particle physics with a discussion not only on the complementarity to other experiments such as LHC but also on completely overwelming outputs compared to those.

LHC

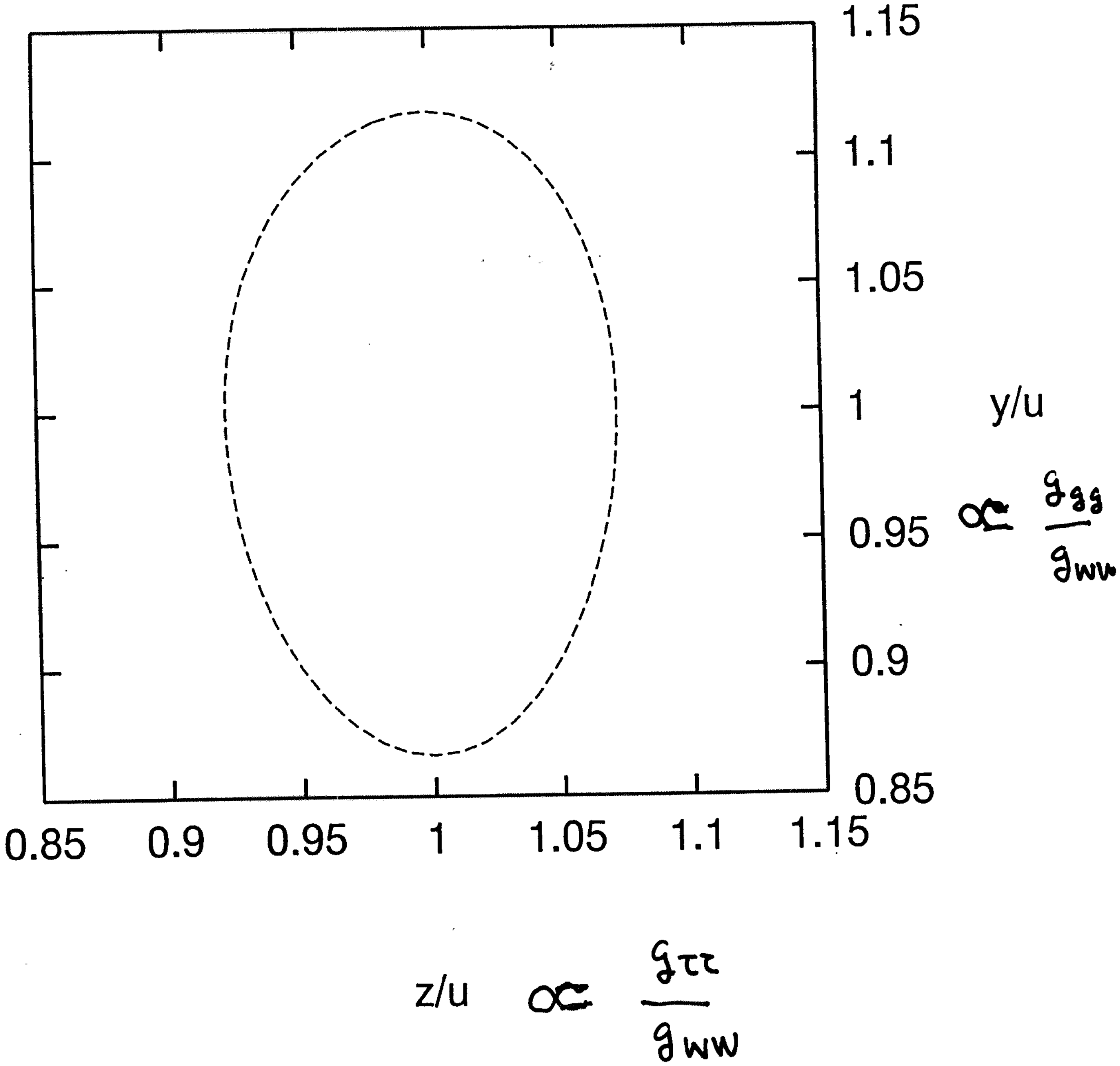
1.15
1.1
1.05
1
0.95
0.9
0.85
y/u
$\propto \frac{g_{gg}}{g_{WW}}$
0.85
0.9
0.95
1
1.05
1.1
1.15
z/u
$\propto \frac{g_{\tau\tau}}{g_{WW}}$

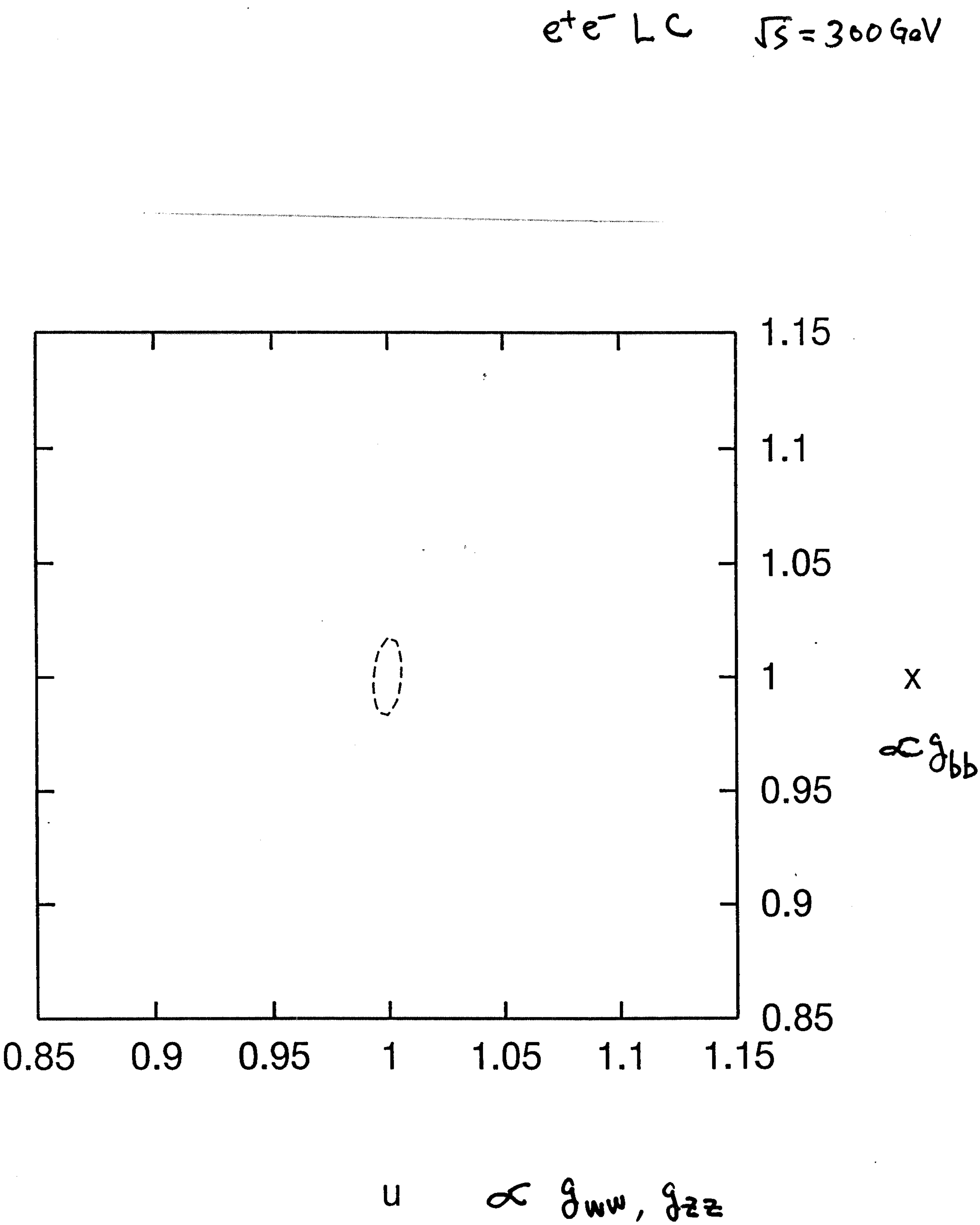

e^+e^- LC $\sqrt{s}=300$ GeV
1.15
1.1
1.05
1
0.95
0.9
0.85
0.85
0.9
0.95
1
1.05
1.1
1.15
x
$\propto g_{bb}$
u
$\propto g_{WW}, g_{ZZ}$

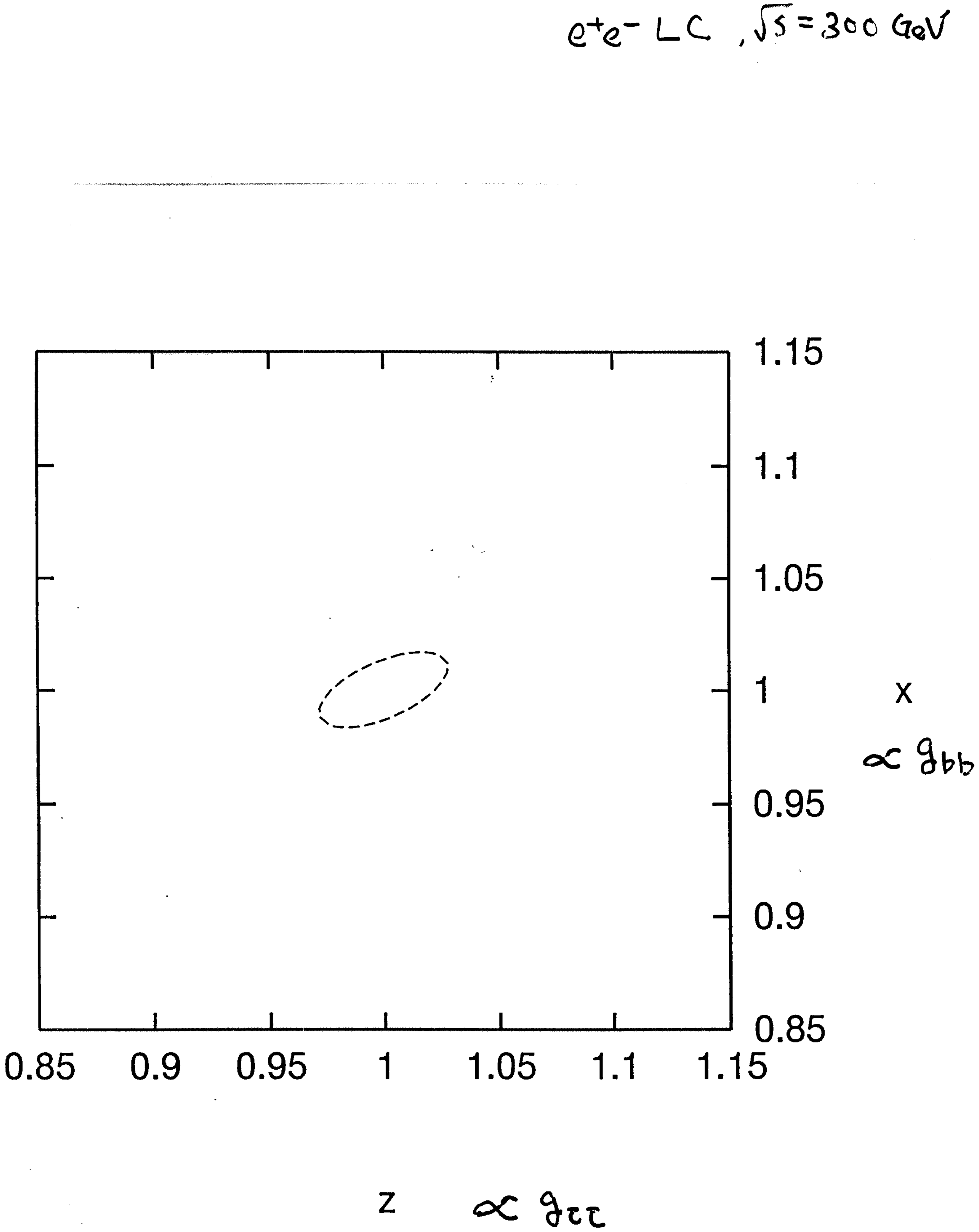
e+e− LC , √s = 300 GeV
1.15
1.1
1.05
1
0.95
0.9
0.85
x ∝ g_bb
0.85
0.9
0.95
1
1.05
1.1
1.15
z ∝ g_ττ

e^+e^- LC, $\sqrt{s} = 300$ GeV

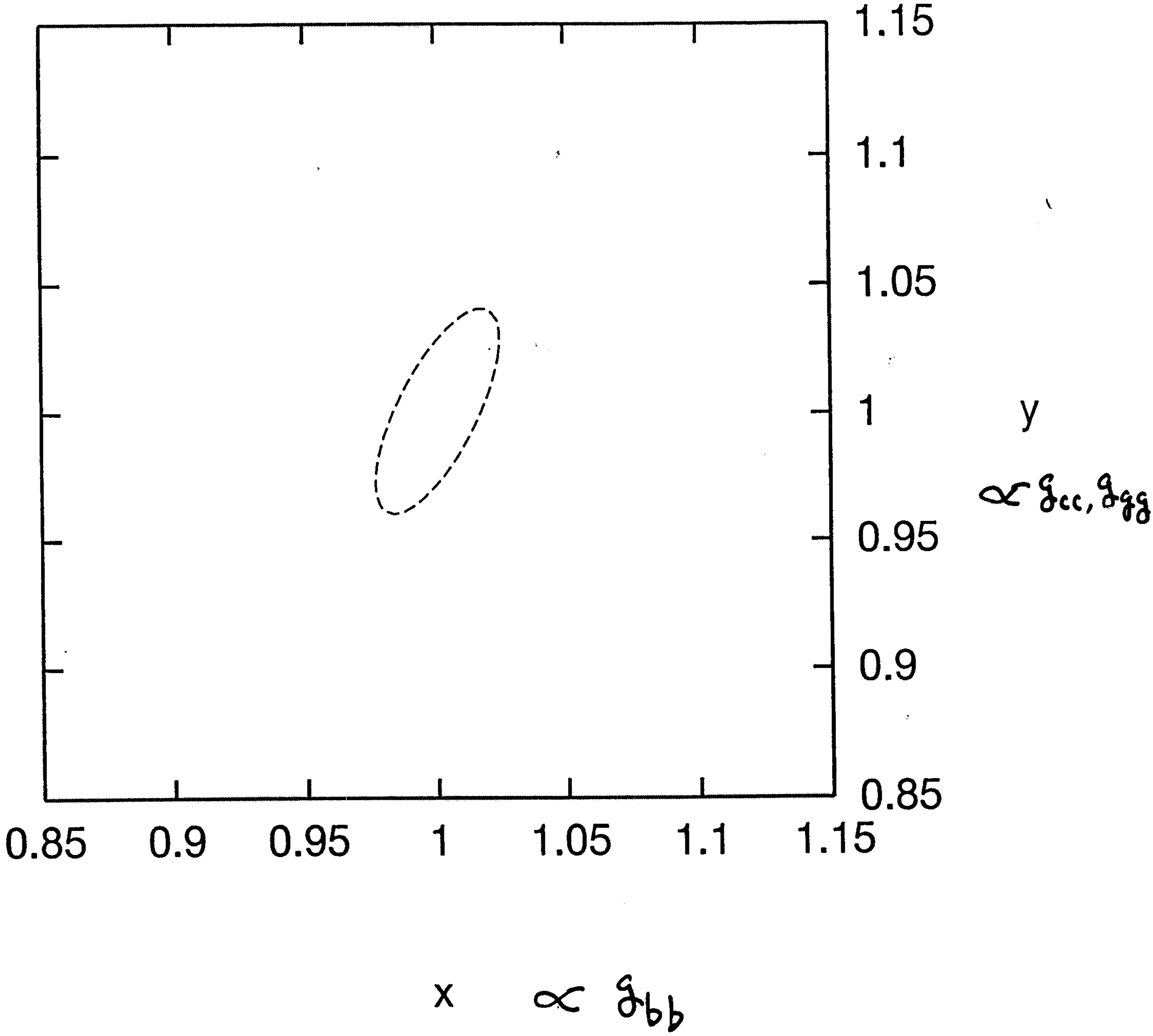

. m_A determination from Branching measurement in MSSM

Decoupling または near-decoupling case では重い Higgs boson は縮退してくる

$$m_A \simeq m_H \simeq m_{H^\pm}$$

もし LHC で軽い Higgs boson 1つだけしか発見できない場合は．重い Higgs boson の質量を間接的に決めることが重要になる。

MSSM における Branching ratio ⟺ m_A の近似式

$$R_{cc+gg/bb} \equiv \frac{B(h\to c\bar{c}) + B(h\to gg)}{B(h\to b\bar{b})} \simeq \left(\frac{m_A^2 - m_h^2}{m_A^2 + m_Z^2}\right)^2 R_{cc+gg/bb}(SM)$$

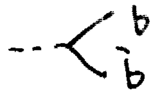

同様な式は $cc+gg/\tau\tau$, $gg/\tau\tau$, WW/bb, $WW/\tau\tau$ でも成立する。

S.Kiyoura・Y.Okada

$$R_{WW/\tau\tau} \equiv \frac{\Gamma(h\to WW)}{\Gamma(h\to\tau\tau)} \simeq \left(\frac{m_A^2 - m_h^2}{m_A^2 + m_Z^2}\right)^2 R_{WW/\tau\tau}(SM)$$

$(\tan\beta \gtrsim 3)$

$\Rightarrow$ m_A を決める。

4 Higgs observable
3 Higgs observable
2 Higgs observable
1 Higgs observable

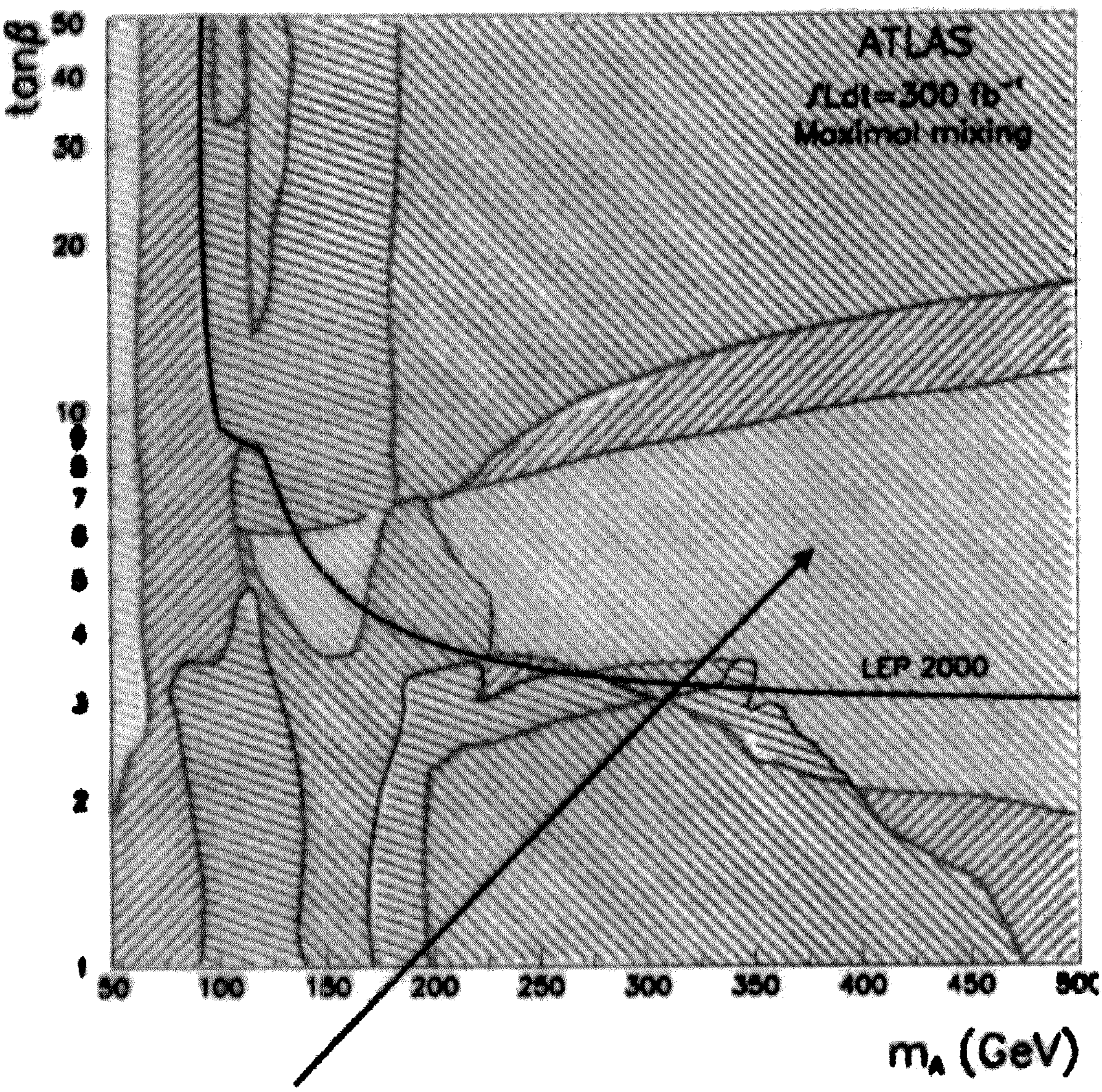

Here:
-- only h observable
-- h ≈ SM Higgs
} → disentangle SM /MSSM ?

$$R_{br} = \frac{B(h\text{->}c\bar{c}) + B(h\text{->}gg)}{B(h\text{->}b\bar{b})}$$

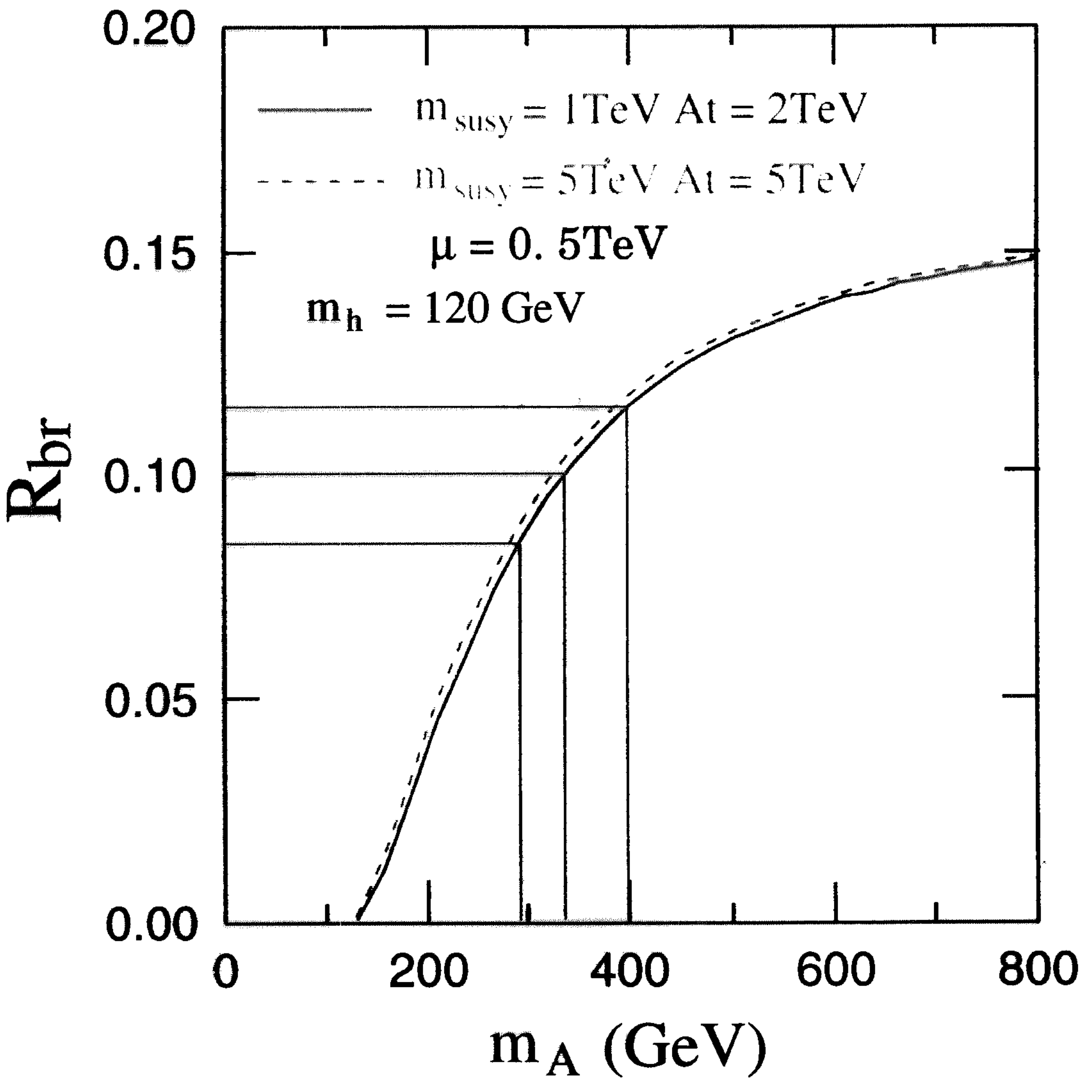

J.Kamoshita,Y.Okada,M.Tanaka, LCWS95 & PLB391(97)124

I.Nakamura, Kawagoe, LCWS95 & PRD54(96)3634, I.Nakamura, LCWS99

Branching ratio の比に対して

LHC (200 fb^{-1})

$$\frac{\Gamma(gg)}{\Gamma(\tau\tau)} \sim 30\% \qquad \frac{\Gamma(WW)}{\Gamma(\tau\tau)} \sim 15\%$$

e^+e^- LC ($\sqrt{s} = 300$ GeV, 500 fb^{-1})

$$\frac{B(cc+gg)}{B(\tau\tau)} \sim 9\% \qquad \frac{B(WW)}{B(\tau\tau)} \sim 7\%$$

$$\frac{B(cc+gg)}{B(bb)} \sim 11\% \qquad \frac{B(WW)}{B(bb)} \sim 9\%$$

三つが独立な量.

LC combined $\sim$ 5 %

$\alpha_s(m_Z)$. 2%

$\overline{m}_b^{MS}(m_b)$. 3%

$\overline{m}_c^{MS}(m_c)$. 5% の不定性から来る理論の誤差を含めてある.

重い Higgs boson や Stop が見つかれば、様々な

パラメーターの決定や MSSM の check ができる。

① m_A が決まる.

Br-measurement ⇒ 一般の 2HDM と MSSM の区別

② Stop Sector が決まる.

$\tilde{t}_2, \tilde{t}_1, A_t$ .. $\tilde{t}_2 \to \tilde{t}_1 h$

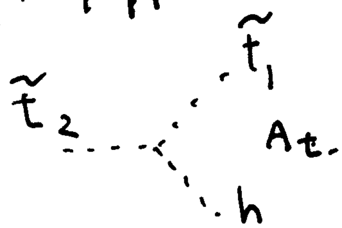

$+ m_A$ (or Br measurement)

Higgs mass の公式から $\tan\beta$ が決まる.

③ m_A, Stop Sector, 他の $\tan\beta$ measurement

- $\tan\beta \Leftarrow$ stau decay $\tilde{\tau}_R \to \tilde{h}\,\tau_L, \tilde{W}\,\tau_R$
- $\tan\beta \Leftarrow$ heavy Higgs decay $H/A \to b\bar{b}$ or $t\bar{t}$, $\tau\bar{\tau}$.
- $\tan\beta \Leftarrow$ chargino/neutralino sector

$\tan\beta$ の consistency check から Higgs Sector が

MSSM か NMSSM かの区別をする

$$m_h^2 \leq \frac{1}{2}\lambda^2 v^2 \sin^2 2\beta + m_Z^2 \cos^2 2\beta + \frac{6}{4\pi^2}\frac{m_t^4}{v^2}\ln\frac{m_{\tilde{t}op}^2}{m_t^2}$$

M. Carena et al hep-ph/0001002

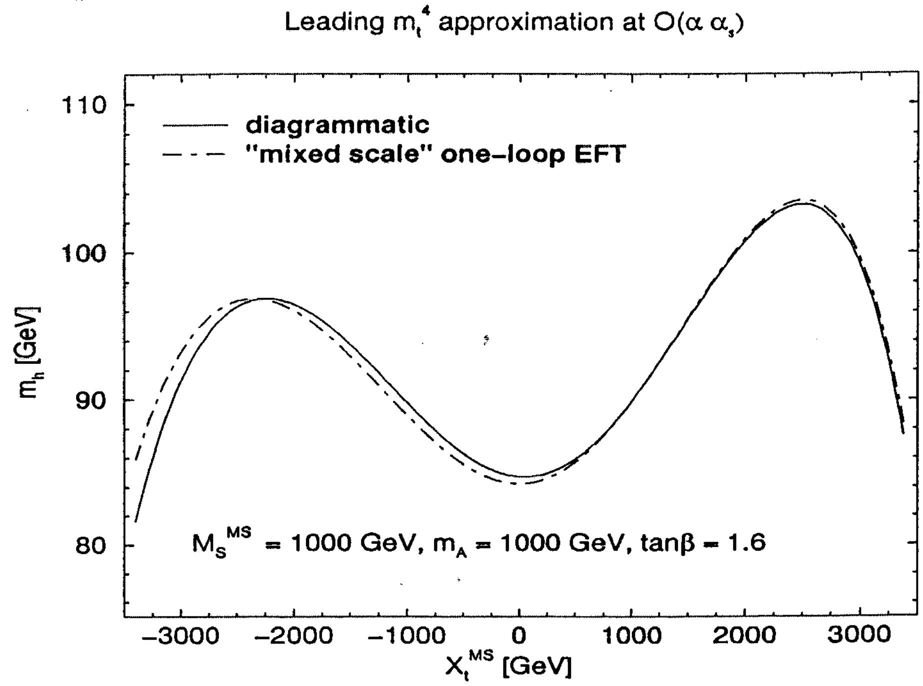

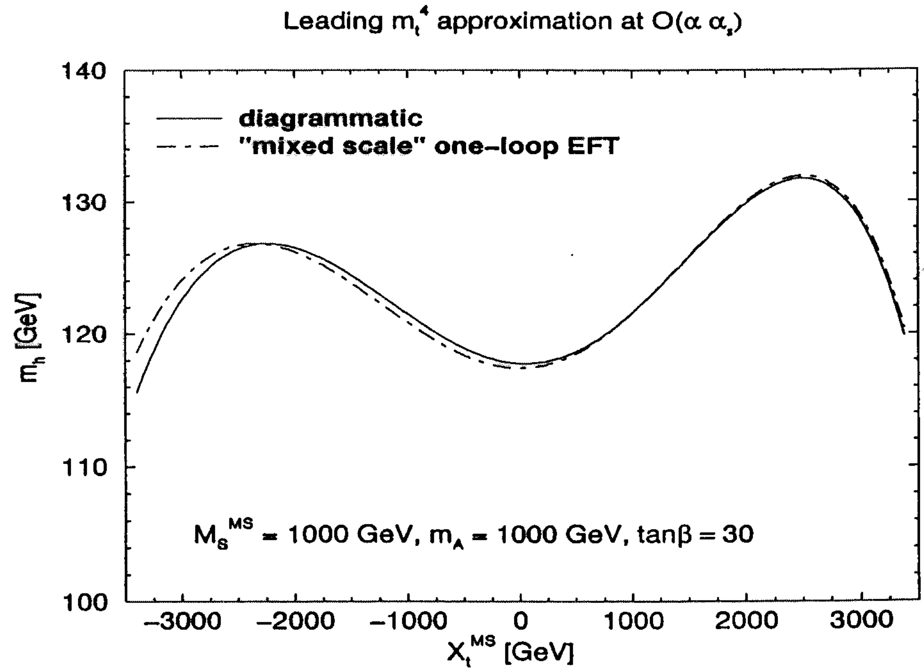

Figure 2. Comparison of the diagrammatic two-loop $\mathcal{O}(m_t^2 h_t^2 \alpha_s)$ result for m_h, to leading order in $\overline{m}_t/\overline{M}_S$ [eqs. (46) and (47)] with the "mixed-scale" one-loop EFT result [eq. (49)]. Note that the latter now includes the threshold corrections due to stop mixing in the evaluation of $\overline{m}_t(M_S)$ in contrast to the EFT results depicted in fig. 1. "Mixed-scale" indicates that in the no-mixing and mixing contributions to the one-loop Higgs mass, the running top quark mass is evaluated at different scales according to eq. (48). See text for further details. The two graphs above are plotted for $\overline{M}_S = m_A = (m_{\tilde{g}}^2 + \overline{m}_t^2)^{1/2} = 1$ TeV for the cases of $\tan\beta = 1.6$ and $\tan\beta = 30$, respectively.

A Bartl et.al PLB 435 (1998) 118

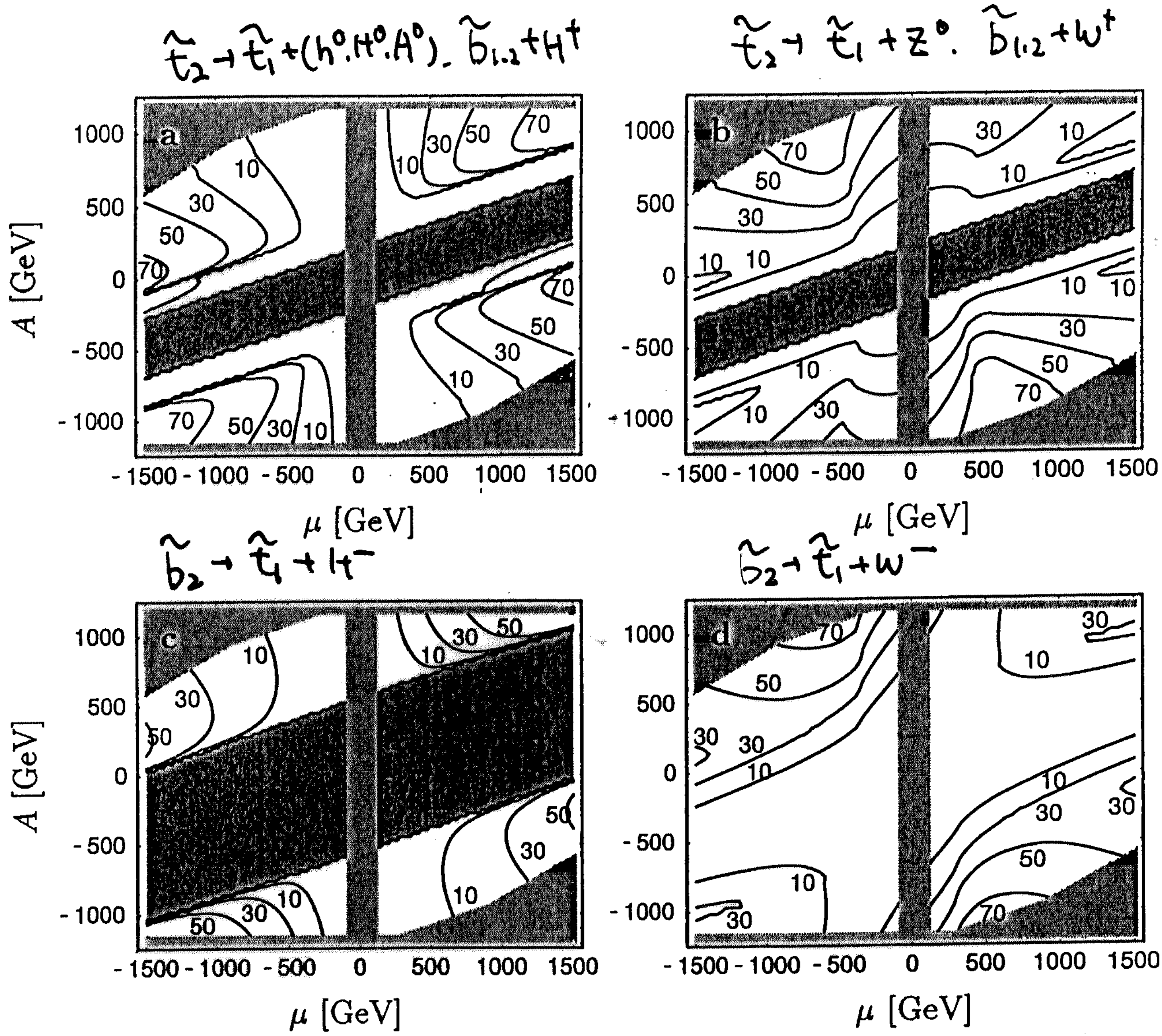

Figure 1: Branching ratios (in %) of $\tilde{t}_2$ and $\tilde{b}_2$ decays in the μ–A plane for $A_t = A_b \equiv A$, $M_{\tilde{Q}} = 500$ GeV, $M_{\tilde{U}} = 444$ GeV, $M_{\tilde{D}} = 556$ GeV, $M = 300$ GeV, $m_A = 150$ GeV, and $\tan\beta = 3$. (a) $\sum \mathrm{BR}[\tilde{t}_2 \to \tilde{t}_1 + (h^0, H^0, A^0),\ \tilde{b}_{1,2} + H^+]$, (b) $\sum \mathrm{BR}[\tilde{t}_2 \to \tilde{t}_1 + Z^0,\ \tilde{b}_{1,2} + W^+]$, (c) $\mathrm{BR}[\tilde{b}_2 \to \tilde{t}_1 + H^-]$, (d) $\mathrm{BR}[\tilde{b}_2 \to \tilde{t}_1 + W^-]$. In the dark grey areas the decays are kinematically not allowed; the light grey areas are excluded by the conditions (i) to (vi) given in the text.

MSSM の軽い CP even Higgs boson の質量公式は SM で ρ parameter の式のような役目を果すことができる.

$$\rho \equiv \frac{M_W^2}{M_Z^2(1-\sin^2\theta_W)} \simeq 1$$

まとめ

① 軽い Higgs boson ($\lesssim 130$ GeV) が MSSM を示唆するシグナル.

② Higgs boson の Branching ratio やその比の決定が MSSM の検証, 模型の区別, パラメーターの決定 (ex. m_A) に重要な意味を持つ.

③ 軽い Higgs boson の性質, 重い Higgs boson の発見. SUSY particle の発見とその性質が解明されて. はじめて. MSSM の十分な検証ができる。